 doi:10.20944/preprints201903.0269.v1

Article

Drilling of sub-100 μm hourglass-shaped holes in Diamond with femtosecond laser pulses

Bosu Jeong[1,3,5], Byunghak Lee[1,5], Jung-Hoon Kim[2], Jung-An Choi[2], Juhee Yang[1], Elena G.Sall[1], Jun Wan Kim[1], Duchang Heo[1], Jinah Jang[3,4], Youngtae Kim[2], and Guang-Hoon Kim[1,*]

[1] Electro-Medical Device Research Center, Korea Electrotechnology Research Institute, 111, Hanggaul-ro, Sangnok-gu, Ansan-si, Gyeonggi-do, Republic of Korea, 15588; bosujeong@keri.re.kr (B.J.); bhlee@keri.re.kr (B.L); zuee@keri.re.kr (J.Y.); elenasall@yandex.ru (E.G.S.); junwankim@keri.re.kr (J.W.K); dcheo@keri.re.kr (D.H.); ghkim@keri.re.kr (G.-H.K.)

[2] GK UP, 64, Deokcheon-ro, Manan-gu, Anyang-si, Gyeonggi-do, Republic of Korea, 14087; kasd0602@naver.com (J.-H.K.); cja2539@naver.com (J.-A.C.); ytee_kim@hotmail.com (Y.K.)

[3] Department of Creative IT Engineering, Pohang University of Science and Technology, 77 Cheongam-ro, Namgu, Pohang, Kyungbuk, Republic of Korea, 37673; jinahjang@postech.ac.kr (J.J.)

[4] School of Interdisciplinary Bioscience and Bioengineering, Pohang University of Science and Technology, 77 Cheongam-ro, Namgu, Pohang, Kyungbuk, Republic of Korea, 37673

[5] The authors contributed equally to this work

* Correspondence: ghkim@keri.re.kr

Abstract: A Micro holes in a diamond are presented by using a homemade femtosecond (fs) Yb:KGW laser. An fs laser source was used emitting pulse duration of 230 fs at 1030 nm wavelength, whereas the spot size amounted to 8.9 μm. Parameters like pulse energy, and pulse number were varied over a wide range in order to evaluate their influence both on the micro hole geometry like hole diameter, circularity, taper angle, and on the drilling quality. Hourglass-shaped micro holes whose diameters decrease and increase again after a certain depth have important applications. The results demonstrate the feasibility of extending the drilling of an hourglass-shaped hole in a diamond sample, which has similar diameters at the hole entrance (92 μm) and exit (95 μm), but a much smaller diameter (28 μm) at a certain waist section inside the hole.

Keywords: Femtosecond laser; Ultrafast laser; Laser micromachining; Laser drilling; diamond

1. Introduction

Diamond is a distinctive material showing variety of utmost properties [1]. It is not only transparent in ultraviolet, visible and infrared areas, they also have high thermal conductivity greater than 20 W/cmK at room temperature. Besides, it has unique radiation stability, chemical inertness, biocompatibility and a number of other important features, which determine numerous applications of this material. The micro holes of diamonds with different diameters and taper angles at different hole depths have various uses. Of these, hourglass-shaped micro holes whose diameters decrease and increase again after a certain depth can be applied to diamond dies for drawing. Laser machining [2] is one important method to produce micro holes and has several advantages such as high spatial resolution, no mechanical drilling-tool wear problem, and good flexible shape, etc. Nanosecond lasers have been used for laser-drilled through-holes. Nonetheless, nanosecond pulses are too long when compared to the duration of the characteristic of laser radiation interaction with the materials. The materials are heated relatively slowly, energy has a lot of time to diffuse into the surrounding area before the affected spot is heated enough for the material removal, which produces a large heat affected zone (HAZ) [3]. Laser processing with femtosecond (fs) laser can ionize a wide range of materials through the high peak power and multi-photon absorption generated in the laser focus region and generate hot plasma at the interface while minimizing the HAZ [4]. Since the material is processed only in the vicinity of the focus point above the ablation threshold, it enables micromachining. High intensities within the focus volume result in multiphoton or tunneling

Preprints (www.preprints.org) | NOT PEER-REVIEWED | Posted: 28 March 2019 doi:10.20944/preprints201903.0269.v1

ionization and subsequent avalanche ionization. Substantial plasma generation and absorption enable the ablation of materials that are normally difficult to ablate by conventional lasers, such as transparent or low-absorption materials. This gives the unique capability of transparent material processing using fs laser [5, 6]. Diamond machining is done by micro-second pulse Nd:YAG and nano-second pulse excimer laser [7]. To the best of the author's knowledge, this paper is the first to study the investigation on a method of drilling of hourglass-shaped holes in a diamond sample using an fs laser, which has an unusually varying diameter with the hole depth.

2. Materials and Methods

The fs laser-induced micro drilling system setup is shown in Figure 1. The optical configuration of the system consists of beam delivery part of fs laser, optical imaging part, and machining part. The system was extended based on the homemade fs Yb:KGW chirped pulse amplification (CPA) laser system [8]. The fs laser has an average power of up to 10 W, a pulse duration of 230 fs, and tunable pulse repetition rate of from 50 kHz up to 500 kHz at the central wavelength of 1030 nm. The output beam is a nearly symmetric Gaussian with $M2 < 1.2$, and the maximum output pulse energy is 200 μJ. The pulse energy is controlled by the combination of a thin-film polarizer (CVI Laser Optics) and a half-wave plate (WPH05M-1030, Thorlabs) mounted on a motorized rotation stage (RSP1/M, Thorlabs). The laser beam is magnified as twice and reflected by a dichroic mirror (M254H45, Thorlabs) and then it is focused at the sample by an objective lens (M Plan Apo NIR 10x, Mitutoyo). Size of the focal spot is about 8.9 μm.

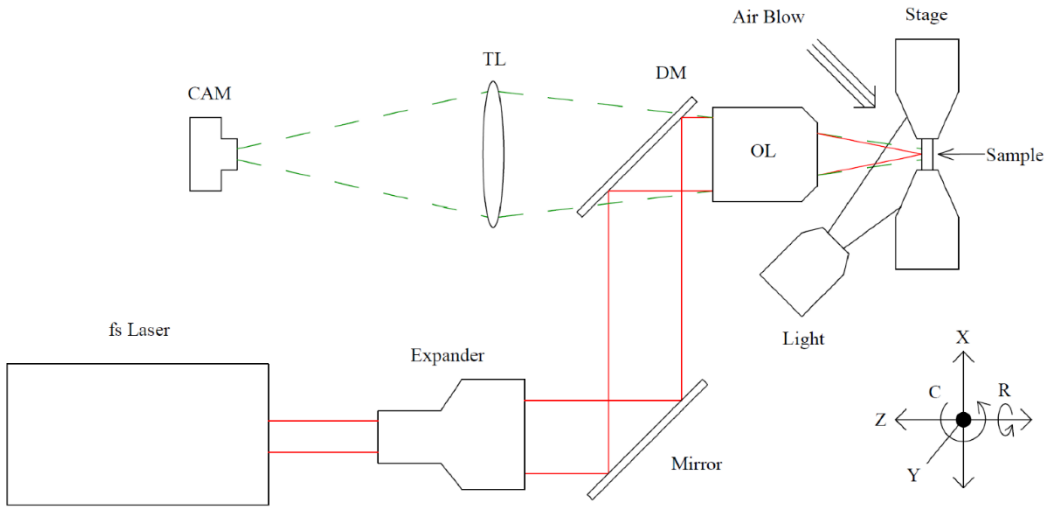

Figure 1. The system setup for the micro hole drilling. CAM: camera, TL: tube lens, DM: dichroic mirror, OL: objective lens. The laser beam and camera signal was depicted in a red solid line and a green dashed line respectively.

The sample was monitored and positioned on the computer-controlled system with 5 axes stages. The system consisted of a high precision 3 linear translation stages (X, Y, Z), and 2 rotation stages (C, R). The X and Y were the directions perpendicular to the direction in which the laser was irradiated in the diamond and Z was the irradiation direction of the laser. One of the rotation stages, C, was used for controlling the incident angle of the laser on the surface of the sample and turning the front and rear of the sample surface. Another rotation stage (R) was used for rotational laser fabrication with a rotation speed of up to 1,000 rpm. An electro-optic modulator in the CPA laser was used as a laser pulse shutter and synchronized to the machining system. After laser machining, the micro-topography of the drilled holes and cut features were characterized by an upright digital microscope. Then the detailed surface quality was measured and characterized by a scanning electron microscopy (SEM). The base materials used in this study were natural diamonds with a range between 360 μm to 420 μm thick mounted on the stainless steel holder supplied by GK UP.

Preprints (www.preprints.org) | NOT PEER-REVIEWED | Posted: 28 March 2019 doi:10.20944/preprints201903.0269.v1

3. Results and discussion

In the beginning, a focal plane position on the sample was determined. The laser spot of the smallest machined area was designated as the focus position of the camera. Figure 2(a) shows the ablation diameter with respect to focal plane position (FPP) on the sample position. In the graph, the ablation diameter increases as the focus area moves away from the FPP. To determine the ablation thresholds for a diamond, which referred to the minimal energy required to initiate material removal, the size of the machining area was compared while varying the laser pulse energy at the focus position. Their diameters were measured and plotted versus laser pulse energy used to ablate the crater. The threshold was estimated from the relationship between the laser fluence and the area of a crater created with a pulse. As shown in Figure 2(b), the ablation test of the sample is investigated and the ablated diameter is plotted as a function of the laser fluence [9]. The extrapolation to zero of the linear fit yields the ablation threshold. The calculated ablation threshold is 60.9 mJ/cm2.

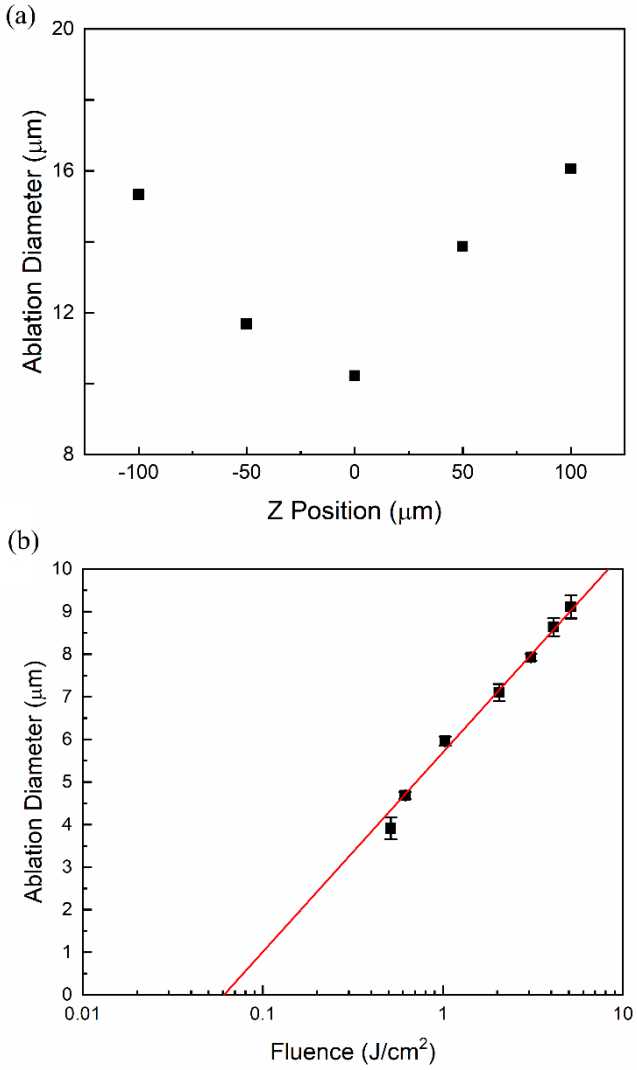

Figure 2. (a) Ablation diameter with respect to focal plane position on the sample position. (b) Ablation threshold measurement for a diamond by using femtosecond (fs) laser.

All studies were performed at a laser repetition rate of 500 kHz, which is below the heat accumulation regime [10]. The FPP was considered as zero when it set on a front material surface. Above or below the front surface, the FPP was considered as positive or negative, respectively. Schematic diagram of FPP is illustrated in Figure 3. The FPP was set to positive to prevent the

Preprints (www.preprints.org) | NOT PEER-REVIEWED | Posted: 28 March 2019 doi:10.20944/preprints201903.0269.v1

processing depth caused by the low numerical aperture of the objective lens used in the experiment and the sample cracking caused by the laser. X translation speed and Z step size optimization were performed to determine the optimal conditions for laser processing.

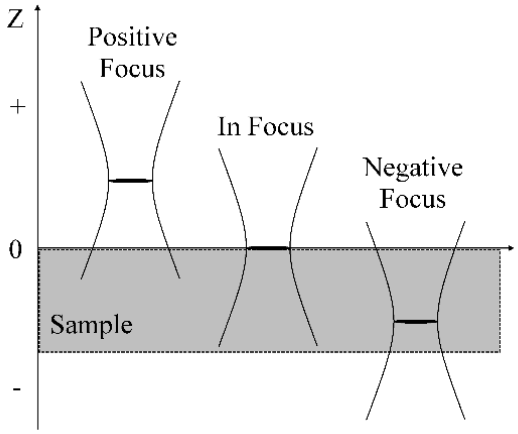

Figure 3. Schematic diagram of focal plane position on the sample.

Figure 4 shows the SEM view of the drilled hole in a diamond. Figure 4(a) shows the geometry of the hole. Figure 4(b) and 4(c) show SEM view of the drilled front and rear hole in a diamond, respectively. The laser output fluence was 3.1 J/cm2. After cleaning the samples, the quality of the machined holes was evaluated. A taper angle of the holes of a diamond was measured as follows:

$$Taper\ angle(2\theta) = tan^{-1}\left(\frac{D_{ent} - D_{exit}}{2t}\right) \quad (1)$$

Where the Dent is entrance hole diameter, Dexit is exit hole diameter, and t is the thickness of the diamond. The holes were 193 μm and 34 μm in diameter at the entrance and exit, and 420 μm in thickness, corresponding to 20.7 degrees of the taper angle of the hole. Figure 4(b) and 4(c) show the drilled holes with good circular geometry for both entrance and exit sides and no micro-crack or thermal damage. It can be observed that with the increase of laser power, the taper angle has been increased slightly along with the increment in both entry and exit diameters of the fabricated micro holes.

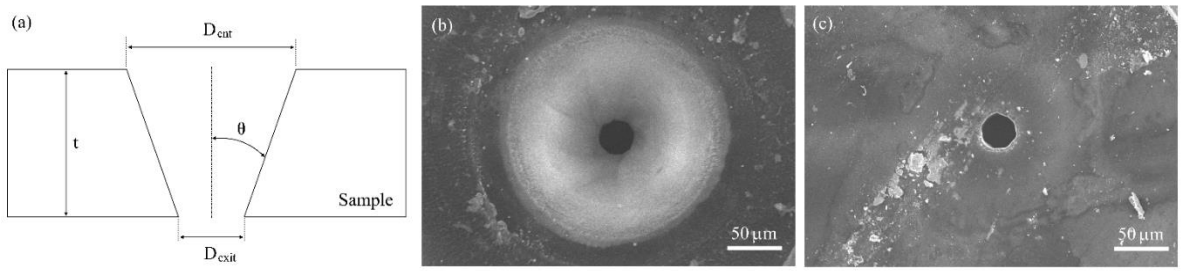

Figure 4. (a) The geometry of the hole. Scanning electron microscope (SEM) view of the drilled hole in a diamond using fs laser: (b) Front view and (c) rear view.

Figure 5(d) shows the geometry of the hourglass-shaped hole. Figure 5(a) and 5(b) show SEM view of the drilled front and rear hole in a diamond. Efforts were made to align the axes of the laser and 5-axis stages to create an hourglass-shaped hole. The front center was aligned with the X, Y, Z stages, and rotation stage (R). After recording the X, Y, Z coordinates, rotating stage (C) was used to show the back surface of the diamond on the camera. Once again, the stages were used to find the back center and coordinates were recorded. The front side of the hourglass was processed

Preprints (www.preprints.org) | NOT PEER-REVIEWED | Posted: 28 March 2019 doi:10.20944/preprints201903.0269.v1

sequentially, and the stage was rotated to the preset coordinates, and then the back side processing was performed. The laser energy used here was 2.1 J/cm2. In order to obtain the taper angle of the front surface and the taper angle of the back surface, the depth to the processed smallest size was obtained through a microscope. Both sizes of the front and rear holes were 92 μm (Dent) and 95 μm (Dexit), respectively. The sizes of the waist hole, Dwaist, was 28 μm and the thickness of the used sample (ttotal) was 420 μm, of which the depth from the inlet to the Dwaist (tent) was 205 μm (the depth from the outlet to the Dwaist (texit) was 215 μm). Both the entrance and the exit side taper angle (θent, θexit) were 16.7 degrees. Smooth surfaces are generally preferred for precision machining. Figure 5(c) shows the SEM view of the surface of the drilled hole in a diamond. Figure 6 shows a ripple for which spacing is generally <200 nm. The orientations of the ripple structures are parallel to each other. Similar ripple structure has been observed in various materials for fs laser drilling [11, 12]. Micromachining with an fs laser creates a clean and smooth hole. Even more exciting is the fact that eliminates the need for post-processing. When drilling with ns and picosecond (ps) lasers, cracks are clearly visible around the exit side of the ns laser perforations, and both the ns and ps laser perforations show thermal damage [13]. The difference is mainly due to the fact that the fs laser pulse length is ultrashort compared to the timescale for thermal diffusion into the material. The accumulation of heat and mechanical stress on the material is greatly suppressed. The ability to drill such holes and hole arrays with consistent regular shape using fs laser is promising and remarkable due to the deterministic nature of fs laser-material interaction. Further improvement of the taper angle and aspect ratio can be achieved by using liquid-assisted rear side drilling [14, 15].

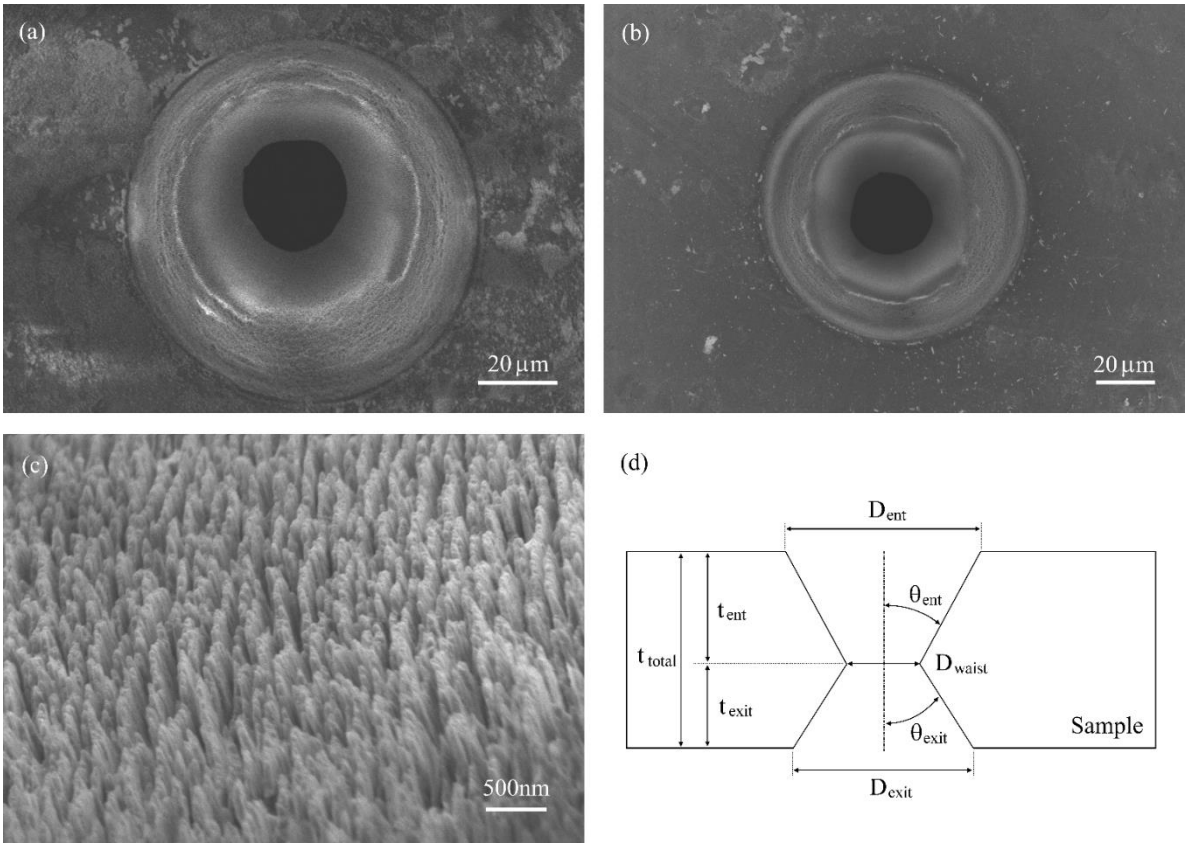

Figure 5. SEM view of the drilled hole in a diamond using fs laser: (a) Front view, (b) rear view, and (c) Entrance side of the hole. (d) The geometry of the hourglass-shaped hole.

4. Conclusions

Fs laser drilling has been carried out with homemade Yb:KGW CPA system. This paper has reported studies on producing small micro holes with unusually varying diameters at different hole

depths like an hour-glass shape hole through fs laser drilling. Drilling experiments focused on the ablation of a natural diamond with 230 fs pulse duration, 500 kHz, and pulse energies from 1.25 μJ to 12.5 μJ. Debris-free micro holes with no thermal damage were achieved for a natural diamond. This laser drilling technique can be applied in the fabrication of microfluidic devices, photonic devices, sensors, and biomedical devices.

Author Contributions: B.J. and G.-H.K. designed the experiment; B.J., B.L., J.Y., J.-H.K., J.-A.C., E.G.S., J.W.K., and D.H. performed the experiment; B.J. and B.L. performed manuscript writing; Y.K. contributed materials; B.J., J.J., and G.-H.K. performed document revising.

Acknowledgments: This research was supported by Korea Electrotechnology Research Institute(KERI) Primary research program through the National Research Council of Science & Technology(NST) funded by the Ministry of Science and ICT (MSIT) (No. 19-12-N0101-64, No. 16-12-N0101-85) and the MIST (Ministry of Science and ICT), Korea, under the ICT Consilience Creative program (IITP-2019-2011-1-00783) supervised by the IITP (Institute for Information & communications Technology Planing & Evaluation).

Conflicts of Interest: The authors declare no conflict of interest.

References

1. M. S. Komlenok; V. V. Kononenko; V. G. Ralchenko; S. M. Pimenov; V. I. Konov. Laser Induced Nanoablation of Diamond Materials. *Physics Procedia* **2011**, 12**,** 37-45
2. V. Tangwarodomnukun; S. Mekloy; C. Dumkum; A. Prateepasen. Laser micromachining of silicon in air and ice layer. *Journal of Manufacturing Processes* **2018**, 36, 197-208
3. J. Ihlemann; B. Wolff; P. Simon. Nanosecond and femtosecond excimer laser ablation of fused silica. *Applied Physics A* **1992**, 54, 363-368
4. K. Venkatakrishnan; N. Sudani; Bo Tan. A high-repetition-rate femtosecond laser for thin silicon wafer dicing. *J. Micromech. Microeng.* **2008**, 18, 075032
5. K. Sugioka; Y. Cheng. Ultrafast lasers—reliable tools for advanced materials processing. *Light: Science & Application* **2014**, 3, e149
6. R. R. Gattass; E. Mazur. Femtosecond laser micromachining in transparent materials. *Nature Photonics* **2008**, 2, 219-225
7. R Windholz; P. A Molian. Nanosecond pulsed excimer laser machining of chemical vapour deposited diamond and highly oriented pyrolytic graphite: Part I An experimental investigation. *Journal of Materials Science* **1997**, 32, 4295-4301
8. G. H. Kim; J. Yang; S. A. Chizhov; E. Sall; A. V. Kulik; V. E. Yashin; D. S. Lee; U. Kang. High average-power ultrafast CPA Yb:KYW laser system with dual-slab amplifier. *Opt. Express* **2012**, 20**,** 3434-3442
9. W. Choi; H. Y. Kim; J. W. Jeon; W. S. Chang; S.-H. Cho. Vibration-Assisted Femtosecond Laser Drilling with Controllable Taper Angles for AMOLED Fine Metal Mask Fabrication. *Materials* **2017**, 10, 212
10. K. Mishchik; K. Gaudfrin; John Lopez. Drilling of Through Holes in Sapphire Using Femtosecond Laser Pulses. *Journal of Laser Micro/Nanoengineering* **2017**, 12, 321-324
11. B. Tan; K. Venkatakrishnan. A femtosecond laser-induced periodical surface structure on crystalline silicon. *J. Micromech. Microeng.* **2006**, 16, 1080
12. S. Gräf; C. Kunz; F. A. Müller. Formation and Properties of Laser-Induced Periodic Surface Structures on Different Glasses. *Materials* **2017**, 10, 933
13. C. Momma; B. N Chichkov; S. Nolte; F. von Alvensleben; A. Tünnermann; H. Welling; B. Wellegehausen. Short-pulse laser ablation of solid targets. *Optics Communications* **1996**, 129, 134-142
14. X. Zhao; Y. C. Shin. Femtosecond laser drilling of high-aspect ratio microchannels in glass. *Applied Physics A* **2011**, 104, 713-719
15. D. J. Hwang; T. Y. Choi; C. P. Grigoropoulos. Liquid-assisted femtosecond laser drilling of straight and three-dimensional microchannels in glass. *Applied Physics A* **2004**, 79, 605-612